Journal of Applied Electrochemistry **33**: 665–674, 2003.

Electrosynthesis of hydrogen peroxide in acidic solutions by mediated oxygen reduction in a three-phase (aqueous/organic/gaseous) system
Part II: Experiments in flow-by fixed-bed electrochemical cells with three-phase flow

E.L. GYENGE and C.W. OLOMAN
Department of Chemical and Biological Engineering, University of British Columbia, 2216 Main Mall, Vancouver, BC, Canada, V6T 1Z4

Received 19 December 2002; accepted in revised form 2 April 2003

Key words: electrosynthesis, fixed bed electrochemical cell, hydrogen peroxide, mediated reduction, redox catalysis

Abstract

The second part of the work concerned with mediated electrosynthesis of H_2O_2 in acidic solutions (pH 3) deals with investigations using divided flow-by fixed bed electrochemical cells operated with co-current three-phase flow (aqueous/organic emulsion and O_2 gas at 0.1 MPa). Graphite felt (GF) and reticulated vitreous carbon (RVC) were evaluated as cathodes at superficial current densities up to 3000 A m^{-2}. Typically, at current densities above 600 A m^{-2} graphite felt yielded higher peroxide concentrations per pass and current efficiencies, most likely due to the almost an order of magnitude higher organic liquid to solid mass transfer capacity for 2-ethyl-9,10-anthraquinone (EtAQ) mediator, that is, 0.13 s^{-1} in the case of GF vs 0.015 s^{-1} for RVC with 39 ppc (pores per cm). Factorial experiments revealed a positive interaction effect between superficial current density and emulsion load with respect to the current efficiency for H_2O_2 electrosynthesis. Thus, at the highest investigated superficial current density of 3000 A m^{-2}, the current efficiency was 84% when the emulsion load was at the highest explored level of 11.7 kg m^{-2} s^{-1}, whilest for the lowest level of emulsion load, 2.8 kg m^{-2} s^{-1}, the current efficiency for H_2O_2 was 18%. Furthermore, the presence of 1 mM cationic surfactant, tricaprylmethylammonium chloride ($CH_3(C_8H_{17})_3N^+Cl^-$, A336), had a positive main effect of about 12% on H_2O_2 current efficiency and there was also a positive synergistic effect between surfactant and emulsion load, estimated at about 7%. The aqueous to organic phase volume ratio, in the range of 0.9/1 and 3/1, had a statistically insignificant effect on the current efficiency for H_2O_2 generation. A decrease of the aqueous to organic phase volume ratio from 3 to 0.9 increased the cell voltage from about 6.5 to 7.3 V.

List of symbols

a	cathode specific surface area (m^2 m^{-3})
A_C	cathode geometric area (m^2)
C	concentration (mol m^{-3}) (Note: for H_2O_2 it refers to the concentration in emulsion)
d	diameter (m)
D	diffusion coefficient (m^2 s^{-1})
f	organic phase volume fraction
F	Faradaic constant (96 500 C mol^{-1})
G	gas load (kg m^{-2} s^{-1})
i	current density (A m^{-2})
K	organic liquid to solid mass transfer coefficient (m s^{-1})
K_{mc}	organic liquid to solid mass transfer capacity (s^{-1})
L	liquid (emulsion) load (kg m^{-2} s^{-1})
n	number of electrons exchanged in the electrochemical reaction
Q_v	volumetric flow rate of the emulsion catholyte (m^3 s^{-1})
S	surfactant (A336) concentration (mM)
u_0	linear emulsion velocity (m s^{-1})
x	coded variable in the factorial regression equation,

$$x = \frac{X_j - \left(\frac{X_{j,\text{low}} + X_{j,\text{high}}}{2}\right)}{\left(\frac{X_{j,\text{high}} - X_{j,\text{low}}}{2}\right)}$$

where X_j is the variable in the factorial design.

Greek symbols

β_L	liquid hold-up
ε	bed porosity
$\Delta\Phi_{max}$	maximum potential drop in the three-dimensional electrode without significant side reactions (V)
κ	ionic conductivity of the emulsion (S m^{-1})
ν_k	kinematic viscosity of the emulsion (m^2 s^{-1})

σ electronic conductivity of the solid matrix (S m^{-1})
τ maximum electroactive bed thickness (m)

Subscripts

0 single phase or initial
eff effective
em emulsion
f graphite fibre
m three-dimensional electrode matrix
ml mass transfer limiting
org organic phase

Abbreviations

A336 Aliquat® 336
EtAQ 2-ethyl-9,10-anthraquinone
GF graphite felt (or fibre bed) electrode
L/L organic/aqueous emulsion
ppc pores per centimetre
RVC reticulated vitreous carbon
TBP tributylphosphate
TBAP tetrabutylammonium perchlorate

1. Introduction

The promising H_2O_2 concentrations obtained in acidic solutions with emulsion mediated electrosynthesis in a batch cell equipped with reticulated vitreous carbon cathodes (e.g., H_2O_2 concentration $\geqslant 0.5$ M at pH 0.9–3. Part I [1]), warranted the investigation of the mediated system in a continuous flow-by electrochemical cell under conditions closer to potential industrial applications. One such application could be the molybdate (MoO_4^{2-}) catalysed acidic peroxide bleaching (e.g., GreenOx process of Kemira Chemicals, Finland). Typical conditions for the latter process in an elemental chlorine free (ECF) bleaching sequence are: 15 kg H_2O_2 t_{pulp}^{-1}, 12% pulp consistency, pH 4.5–5, 0.45 kg Na_2MoO_4 t_{pulp}^{-1}, 90 °C, and 3 h bleaching time [2]. The required peroxide load corresponds to a H_2O_2 concentration in solution of about 0.06 M. For a total chlorine free (TCF) bleaching the required H_2O_2 load is higher, that is, 52.5 kg H_2O_2 t_{pulp}^{-1} [2], corresponding to a H_2O_2 concentration in solution of about 0.2 M.

Based on the preliminary electrolysis conducted in 2 M Na_2SO_4 acidified with glacial acetic acid to pH 3 [1], it is expected that the H_2O_2 concentration and pH requirements of the molybdate activated peroxide bleaching could be met by the proposed redox catalytic system for electrosynthesis of H_2O_2.

The objective of Part II of the present work was to study the interplay among electrode kinetic aspects, emulsion structure and three-phase (L/L/G) flow hydrodynamics in relation to emulsion mediated peroxide electrosynthesis in fixed-bed flow-by cells.

2. Experimental details

Two fixed-bed electrochemical cells were used with 0.15 and 0.51 m effective length, respectively. The corresponding superficial areas were 3.3×10^{-3} m^2 and 26.7×10^{-3} m^2 (Figures 1(a) and (b), respectively). Both cells were operated in flow-by mode with co-current upward three-phase L/L/G flow in the cathode compartment.

The shorter cell (Figure 1(a)) was equipped with either graphite felt (Carborundum Co., 99% C content) or reticulated vitreous carbon (12 and 39 pores per cm, ppc, respectively, ERG Materials and Aerospace) three-dimensional cathodes of 4.5 mm thickness. The highest

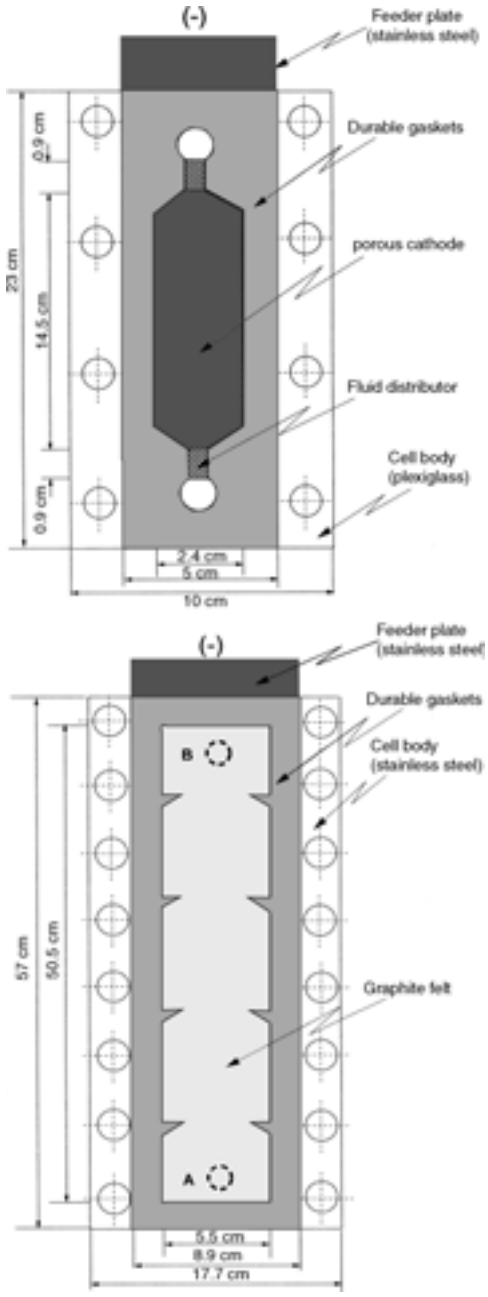

Fig. 1. Front view of the cathode compartment. Legend: (a) 'short' cell, (b) 'long' cell. In (b), A ≡ inlet and B ≡ outlet.

Table 1. Physico-chemical characteristics of the reticulated vitreous carbon (RVC) and graphite felt (GF) electrodes

Property	GF*	RVC 39 ppc	RVC 12 ppc
Specific surface area/m^2 m^{-3}	16 000	6560	1800
Porosity	0.92	0.95	0.78
Electronic conductivity of the matrix/S m^{-1}	23	62	122

* Data corresponding to 38% compression.

current applied to the 'short' cell (effective length 0.15 m) was 22 A. The second flow cell employed in the present work, sometimes referred to as the 'long' cell (Figure 1(b)), was equipped with graphite felt cathode (4.5 mm compressed thickness). The highest current applied to the 'long' cell (effective length 0.51 m) was 27 A.

Table 1 compares certain physico-chemical properties for the RVC and graphite felt electrodes. The specific surface area (S_{GF}/m^2 m^{-3}) and electronic conductivity (σ_{GF}/S m^{-1}) of the compressed graphite felt matrix were calculated with the following formula [3]:

$$S_{GF} = \frac{4(1-\varepsilon)}{d_f} \quad (1)$$

and

$$\sigma_{GF} = 10 + 2800\left(1 - \frac{\varepsilon}{\varepsilon_0}\right)^{1.55} \quad (2)$$

where d_f is the diameter of the graphite fibre (20 μm), ε_0 and ε is the porosity of the graphite felt corresponding to the initial (uncompressed) and compressed electrodes, respectively, 0.95 and 0.92.

The specific surface area of the reticulated vitreous carbon electrodes was obtained from literature [4], while the electronic conductivities and porosities were experimentally measured [5].

Table 1 shows that graphite felt possessed almost an order of magnitude higher specific surface area and about a six times lower electronic conductivity as compared to RVC 12 ppc. The specific surface area influences the mass transfer capacity of the employed three-dimensional electrodes while the electronic conductivity of the matrix has an effect on the potential and current distribution. Therefore, the differences in physico-chemical characteristics presented by Table 1 will play a major role in the overall performance of the three electrodes used in the present work.

Figure 2 shows the arrangement of all the cell components on both the cathode and anode side exemplified for the case of the 'short' cell. The same arrangement was used for the 'long' cell with two exceptions: first, the cell body was made of stainless steel for the long cell and plexiglass in the case of the short cell, respectively; secondly, the former was equipped with an additional compartment to allow for cooling water circulation at the back of the cathode current feeder. The anode and cathode compartments were separated by a Nafion® 350 membrane supported by a plastic screen on the anode side, which also acted as a spacer and static turbulence promoter. A dimensionally stable O_2 anode (DSA) of 1 mm thickness was used. The cell assembly was uniformly compressed using a torque wrench.

The catholyte was an aqueous/organic emulsion with phase volume ratios between 3 /$1_{(v/v)}$ and 0.9/$1_{(v/v)}$. The aqueous phase was composed of 1 M Na_2SO_4 acidified with glacial acetic acid to an initial pH of 3. The organic phase was tributylphosphate (TBP) with supporting electrolyte (tetrabutylammonium perchlorate, TBAP), mediator (2-ethyl-9,10-anthraquinone, EtAQ) and cat-

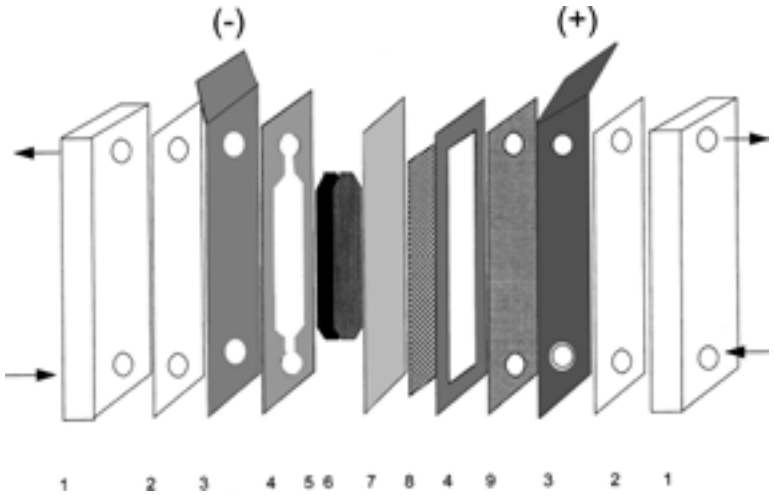

Fig. 2. Set-up and components of the fixed-bed cell. Legend: (1) Plexiglass or stainless steel cell body, (2) rubber gasket, (3) stainless steel current feeder, (4) Durabla® gaskets, (5) graphite paper (0.3 mm thickness, used with the RVC cathode only), (6) three-dimensional (fixed-bed) cathode (graphite felt or reticulated vitreous carbon), (7) Nafion® 350, (8) plastic screen, (9) dimensionally stable O_2 anode.

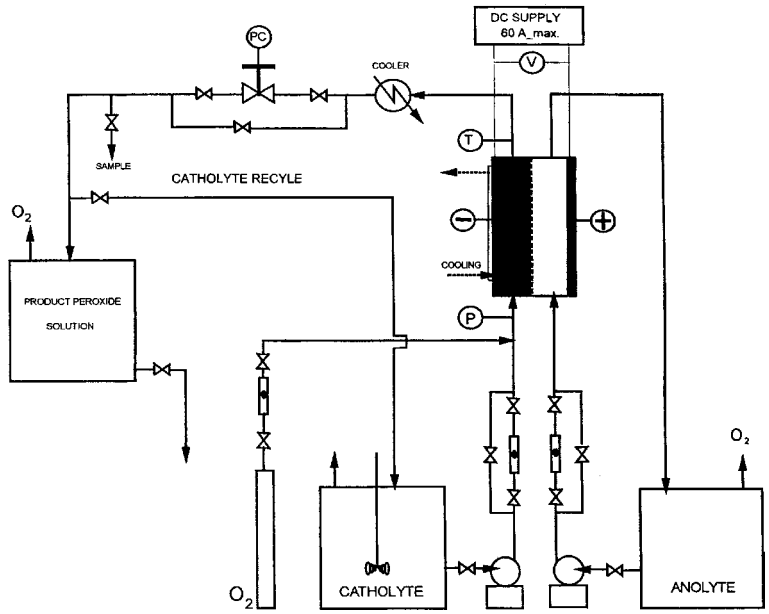

Fig. 3. Experimental set-up for the mediated electrosynthesis of H_2O_2 employing a flow-by fixed-bed electrochemical cell.

ionic surfactant (tricaprylmethylammonium chloride, A336) dissolved in it. The organic chemicals were obtained from Sigma-Aldrich Co. The inorganic chemicals were purchased from Fisher Scientific. In all experiments deionized water was used with a specific conductivity of 200 μS m^{-1}.

Figure 3 shows the layout of the experimental set-up including the electrochemical cell. The catholyte feed tank stored 16 liter of emulsion with the desired phase volume ratio. The two-phases were mixed continuously using a mixer equipped with a bow-tie coil paddle. The anolyte feed tank contained up to 30 litre of 0.5 M Na_2SO_4 at pH 3.0 (adjusted with glacial acetic acid).

A diaphragm pump with polypropylene head and a flow range 0.8–158 cm^3 min^{-1} (LE 91T, LMI Milton Roy) was employed for pumping the L/L emulsion. As shown by Figure 3, O_2 gas flow was fed into the emulsion before the electrochemical cell. Thus, the three-dimensional cathode of the electrochemical cell was operated with co-current upward three-phase L/L/G flow. In parallel with the catholyte flow, the anolyte was pumped through the anode compartment in upward flow at a constant rate of 55 cm^3 min^{-1}. The fluid outlet temperature of the 0.51 m long cell was kept constant at about 300 K by cooling the back of the stainless steel cathode feeder plate with cold tap water.

After exiting from the electrochemical cell the product catholyte was sampled for H_2O_2 content as determined by $KMnO_4$ titration [6]. The catholyte was collected in a storage tank allowing for the separation of phases and disengagement of the excess O_2 gas. In the case of complete catholyte recycle, instead of collecting the peroxide containing solution in the storage tank, the catholyte emulsion was recycled in the electrochemical cell (Figure 3).

3. Results and discussion

3.1. *Cathode selection*

In batch experiments RVC was the preferred cathode material [1]. However, in the case of the flow cell the issue of the three-dimensional cathode has to be revisited due to different hydrodynamic and mass transfer constraints. Using the 0.15 m effective length flow cell (Figure 1(a), Section 2) three cathode materials were tested, RVC 12 and RVC 39 pores per cm and graphite felt, respectively (Table 1). The H_2O_2 concentration obtained per one pass and the corresponding current efficiency was compared for an emulsion composed of a 2.1/1 volume ratio of aqueous to organic phase (Figure 4(a) and 4(b)). The current efficiency was calculated with the formulae:

$$\mathrm{CE} = \frac{nFQ_{\mathrm{V}}C_{\mathrm{H_2O_2}}}{iA_{\mathrm{C}}} \times 100 \qquad (3)$$

where A_{C} is the cathode geometric area (m^2), $C_{\mathrm{H_2O_2}}$ the peroxide concentration per pass in the emulsion (mol m^{-3}), F the faradaic constant (C mol^{-1}), i the cathode superficial current density (A m^{-2}), n the number of electrons (=2) and Q_{V} the volumetric flow rate of the emulsion catholyte (m^3 s^{-1}).

The flow rates were 4.5×10^{-7} m^3 s^{-1} for the L/L emulsion and 1.98×10^{-6} m^3 s^{-1} at STP for O_2 gas. The corresponding liquid load was 4.25 kg m^{-2} s^{-1} with a gas load of 2.6×10^{-2} kg m^{-2} s^{-1}, assuring a liquid continuous flow regime [7].

Figures 4(a) and (b) show that the H_2O_2 concentration per pass and current efficiency was generally higher for graphite felt than for the reticulated vitreous carbon electrodes. Table 2 indicates that among the

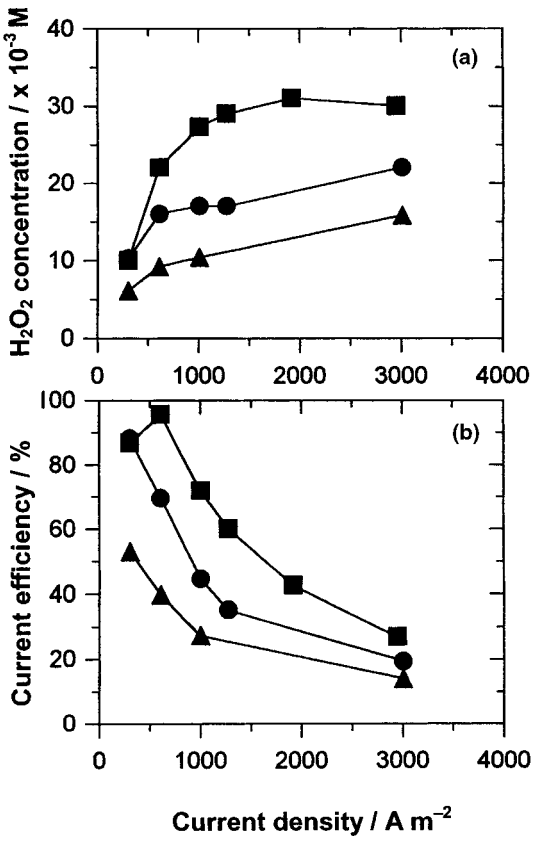

Fig. 4. Comparison between graphite felt (GF) and reticulated vitreous carbon (RVC) cathodes used in the flow-by cell for mediated electrosynthesis of H_2O_2 at pH 3. Organic phase: TBP–0.2 M EtAQ–0.1 M TBAP, aqueous phase: 1 M Na_2SO_4 (acidified to pH 3), 10^{-3} M A336 per emulsion. Phase volume ratio: $2.1/1_{aq/org}$. Emulsion load: 4.25 kg m^{-2} s^{-1}, O_2 load 0.026 kg m^{-2} s^{-1} (at STP), pressure 0.1 MPa. 308 K. Legend: (a) H_2O_2 concentration per pass, (b) current efficiency for H_2O_2. Legend: (■) graphite felt, (●) reticulated vitreous carbon 39 ppc, (▲) reticulated vitreous carbon 12 ppc.

investigated electrodes graphite felt was characterized by the highest mass transfer capacity and limiting superficial current density; for example, almost on order of magnitude higher mass transfer capacity as compared to RVC with 39 ppc and a superficial limiting current density of 1470 A m^{-2} on graphite felt in comparison to only 550 A m^{-2} in the case of RVC (39 ppc). The calculation procedure of the liquid–solid mass transfer coefficients and capacities, maximum electroactive bed thickness and limiting superficial current densities for the three electrodes under study, is detailed in Appendix 1.

Figure 4(b) reveals that at current densities below the mass transfer limited values for the respective electrodes, the H_2O_2 current efficiencies were 60 to 95%; for example, for graphite felt at 600 A m^{-2} a 95% current efficiency was obtained. At 600 A m^{-2} the RVC electrodes, in conformity with their lower mass transfer limited current densities (Table 2), yielded a current efficiency of 70% (RVC with 39 ppc), and 40% efficiency (RVC with 12 ppc), respectively.

For the employed hydrodynamic conditions the maximum electroactive bed thickness for graphite felt, which can operate at the limiting current density without significant side reactions, (e.g., H_2O_2 electroreduction) is only a small fraction (e.g., less than one tenth) of the nominal bed thickness (Table 2). This aspect gains importance at superficial current densities above approximately 1500 A m^{-2}, where the H_2O_2 concentration per pass levels off or decreases as a result of the secondary reaction of H_2O_2 electroreduction over much of the nominal bed thickness (Figure 4(a)).

Using the graphite felt cathode, comparative experiments were also performed with and without the mediator EtAQ present in the organic phase. In the absence of EtAQ (i.e., direct electroreduction of O_2 in the emulsion electrolyte) for superficial current densities greater than 300 A m^{-2} the H_2O_2 concentration per pass and the corresponding current efficiency were significantly lower than for the mediated system (i.e., with EtAQ present). At 1950 A m^{-2} the current efficiency was 43% with EtAQ mediator (Figure 4(a)) while under the same conditions but without organic redox mediator, the current efficiency was only 15% [5].

Based on the higher current efficiency for peroxide electrosynthesis (Figure 4(a) and (b)), graphite felt was retained as the electrode material of choice for the system under investigation.

3.2. *Factorial experimental design*

Employing a graphite felt cathode in the 0.15 m effective length cell, a full factorial design was performed involving four variables at two levels plus one centerpoint (i.e., $2^4 + 1$ design) (Table 3). The variables were: superficial current density, emulsion load, aqueous to organic phase volume ratio and cationic surfactant (A336) concentration. The O_2 gas load, outlet reactor pressure and temperature were kept constant at 1.45×10^{-2} kg m^{-2} s^{-1}, 0.1 MPa and 313 K, respec-

Table 2. Estimated organic liquid-to-solid mass transfer coefficient, mass transfer capacity, maximum electroactive bed thickness and superficial limiting current density for EtAQ reduction in acid emulsion using a flow-by cell (Appendix 1)
Emulsion load 4.25 kg m^{-2} s^{-1}; O_2 load at STP: 0.026 kg m^{-2} s^{-1} (Figure 4)

Electrode	Mass transfer coefficient/m s^{-1}	Mass transfer capacity/s^{-1}	Maximum electroactive bed thickness/m	Limiting superficial current density/A m^{-2}
GF	2.4×10^{-5}	1.3×10^{-1}	3×10^{-4}	1470
RVC 39 ppc	7.7×10^{-6}	1.6×10^{-2}	9×10^{-4}	550
RVC 12 ppc	3.1×10^{-6}	1.8×10^{-3}	3×10^{-3}	180

Table 3. Variables and their respective levels used in the factorial study of EtAQ mediated H_2O_2 electrosynthesis at pH 3 using the 0.15 m effective length flow-by cell

Variable (symbol, units)	Level		
	Low (−)	Centre (0)	High (+)
Superficial current density, i/A m^{-2}	1000	2000	3000
Emulsion load, L/kg m^{-2} s^{-1}	2.8	6.9	11.7
Aqueous/organic phase volume ratio, R	0.9	2.1	3
A336 concentration, S/mM$_{\text{per emulsion}}$	0	0.5	1

tively. Also, the concentration of redox catalyst EtAQ 0.2 M, supporting electrolyte TBAP 0.1 M, and aqueous electrolyte Na_2SO_4 1 M (acidified with acetic acid to $pH_{initial}$ 3), remained the same throughout the factorial experiments.

The H_2O_2 concentration per single pass and current efficiency for the seventeen experiments are summarized in Table 4. According to entry 13 (Table 4) for a current density of 3000 A m^{-2} a current efficiency for H_2O_2 as high as 84% was obtained providing the surfactant and emulsion load were at their respective 'high' levels whilest the aqueous/organic phase volume ratio was set to its 'low' level (Table 3). It is important to note in this context the significance of surfactant presence. Under similar conditions but without A336, the current efficiency was 65% (entry 8, Table 4).

Table 4. Factorial experimental results corresponding to the design composed of four variables at two levels and one centrepoint (i.e., $2^4 + 1$)
Cathode: graphite felt

No.	i	L	R	S	H_2O_2 concentration* /$\times 10^{-3}$ M	Current efficiency† /%
1	−	+	+	+	12	87
2	−	+	−	−	11 ± 0.5	80 ± 3
3	−	+	+	−	10	72
4	+	+	+	−	23	55
5	+	−	+	−	26	15
6	−	−	−	−	34	60
7	+	+	+	+	32	77
8	+	+	−	−	27	65
9	−	−	−	+	40	70
10	+	−	+	+	34	19
11	−	−	+	+	38	63
12	−	+	−	+	14	100
13	+	+	−	+	35	84
14	0	0	0	0	31 ± 0.9	66 ± 1.8
15	+	−	−	+	30	18
16	+	−	−	−	29	16
17	−	−	+	−	35	62

† Average factorial response for current efficiency 59.5%; pooled standard deviation ±2.3%.

* Average factorial response for H_2O_2 concentration 27×10^{-3} M; pooled standard deviation $\pm 9 \times 10^{-4}$ M.

Generally, the current efficiency for H_2O_2 increased with the emulsion load, for example, compare entries 12 and 9 in Table 4. The peroxide concentration per pass had the opposite behaviour.

The main and two-factor interaction effects were calculated with the Jass® 2.1 software and are given in Table 5.

Table 5 shows that the emulsion catholyte load exerted the strongest positive main effect on the apparent current efficiency for H_2O_2 (i.e., 37%), followed by the surfactant at 12%. The superficial current density had a significant negative main effect on current efficiency (i.e., −31%). Interestingly, the phase volume ratio exerted only a small main effect under the present conditions, bordering statistical insignificance (i.e., −5%). In other words, decreasing the aqueous/organic volume ratio (Table 3), on average did not significantly improve the current efficiency (e.g., compare entries 9 and 11, or 10 and 15, Table 4).

The latter finding could be explained based on the fact that the electrochemical reaction zone is situated at the proton-rich organic/aqueous/solid boundary (see Part I, [1]) and not in the bulk organic phase. Therefore, increasing the organic phase volume on the expense of the aqueous phase does not significantly improve the performance of the system. Furthermore, from the point of view of energy consumption a lower aqueous/organic phase volume ratio gives higher cell voltage, for example, 6.5 V at 1000 A m^{-2} for a ratio of 3/1 and 7.3 V for a ratio of 0.9/1.

The main effects of the emulsion load and current density must be interpreted in conjunction with the strong positive interaction factor between these two variables (Table 5). At high current density (3000 A m^{-2}) increasing the emulsion load to its high level of

Table 5. Main and interaction effects corresponding to the ($2^4 + 1$) factorial experimental design

Effects		H_2O_2 concentration* /$\times 10^{-3}$ M	Current efficiency† /%
Main	i	5.3	−30.6
	L	−12.8	37
	R	−1.0	−4.6
	S	5.0	11.6
Two-factor interaction	iL	12.3	16.1
	iR	−0.3	1.1
	iS	1.5	0.1
	LR	−1.3	−4.2
	LS	0.5	7.4
	RS	0.5	−1.1
Three-factor interaction	iLR	−0.8	−0.1
	iLS	1.5	1.4
	iRS	1.5	2.4
	LRS	−0.5	0.6

* Standard error of H_2O_2 concentration effect $\pm 1.9 \times 10^{-3}$ M.

† Standard error of current efficiency effect ±4.8%.

11.7 kg m^{-2} s^{-1} enhanced the current efficiency by an average of 16%. The main effect of emulsion load and its interaction with current density is a reflection of the residence time in the flow cell coupled with mass transfer effects. For 'high' emulsion load the residence time is smaller than in the case of 'low' catholyte load level, yielding lower H_2O_2 concentrations per pass with relatively minor contribution of side reactions (Table 4). On the other hand, at 'low' emulsion load (2.8 kg m^{-2} s^{-1}) the mass transfer capacity for EtAQ transport to the electrode is small inducing a reduced limiting superficial current density of about 800 A m^{-2} (calculated with the procedure given by Appendix 1). Therefore, in the factorial experiments for the 'low' emulsion load increasing the current density from 1000 to 3000 A m^{-2} decreased the current efficiency below 20%, as shown by entries no. 5, 10, 15 and 16 in Table 4. At 'high' load on the other hand, the EtAQ mass transfer is enhanced, consequently at 3000 A m^{-2} the observed current efficiencies were in the range of 55–84%.

Regarding the cationic surfactant, in addition to its main effect a positive interaction was found between surfactant and emulsion load (i.e., 7%, Table 5). This result suggests that A336 was more effective at high catholyte emulsion load. Indeed, comparing entries 4 and 7 in Table 4 shows that the presence of 1 mM A336 in the emulsion improved the current efficiency from 55 to 77% when the emulsion load was 11.7 kg m^{-2} s^{-1}, while under similar conditions but at 'low' liquid load, the presence of A336 had a lesser effect (compare entries 5 and 10, Table 4). The rest of the interaction effects were statistically insignificant (Table 5).

The average factorial response for peroxide current efficiency was 59.5%. The curvature effect for current efficiency, calculated as the difference between the centerpoint and the average of factorial response, was 6.5 ± 5%. This shows only a small degree of system nonlinearity in the range of investigated variables.

Based on the factorial experiments, neglecting the statistically insignificant values, the regression equation for peroxide current efficiency can be written as:

$$CE_{reg}(\%) = 59.5 - 15.3\,x_i + 18.5\,x_L + 5.8\,x_S + 8.05\,x_i x_L + 3.7\,x_L x_S \qquad (4)$$

where the coded variables x_j are expressed as

$$x_i = \frac{i - 2000}{1000} \quad x_L = \frac{L - 7.25}{4.41} \quad x_S = \frac{S - 0.5}{0.5}$$

where i is the current density (A m^{-2}), L the emulsion load (kg m^{-2} s^{-1}) and S the surfactant concentration per emulsion (mM).

3.3. *Influence of flow regimes*

Both the factorial and parametric experiments presented so far were performed in liquid continuous (bubble flow) regime. Therefore, it was of interest to study the influence of O_2 gas load and implicitly the effect of different flow regimes, on the performance of the multiphase electrosynthesis. The H_2O_2 concentration per single pass was followed as a function of increasing gas loads covering a wide range of regimes from bubble (liquid continuous) to pulsating (gas continuous) flow, corresponding to liquid/gas load ratios from 438 to12, respectively (Figure 5). The rest of the variables were kept constant (see legend, Figure 5).

Interestingly, at 3000 A m^{-2} the O_2 load had virtually no influence on the H_2O_2 concentration. It has been established that increasing the gas load decreases the liquid hold-up in graphite felt electrodes [8]. For the present case, the transition from liquid continuous to gas continuous regime is estimated to decrease the liquid hold-up by about 18% (i.e., from 0.85 to 0.7) [5]. It is possible that the negative effect of lower liquid hold-up at high gas load is compensated by a higher O_2 mass transfer capacity and homogeneous reaction rate between anthrahydroquinone and O_2, which could be the rate determining step at the high cathode overpotential corresponding to 3000 A m^{-2}.

3.4. *Catholyte recycle: 0.51 m effective length flow-by cell*

The mediated peroxide electrosynthesis in acidic solutions was further evaluated using the 0.51 m effective length cell (see Section 2). The experimental conditions were selected based on the know-how gained with the factorial experiments. Thus, the catholyte was composed of a 3/1 volume ratio of aqueous and organic phases, with a cationic surfactant concentration per emulsion of 1 mM. The emulsion flow rate was set to the highest achievable flow with the employed pump (Section 2), that is, 2.5×10^{-6} m^3 s^{-1}, corresponding to a load of 10 kg m^{-2} s^{-1}. The gas load was 0.088 kg m^{-2} s^{-1}, assuring a liquid continuous flow regime. The total recirculated emulsion volume was 3.5 l, which passed all through the reactor in about 24 min. The reactor was operated in galvanostatic mode at a cathode superficial current density of 1000 A m^{-2} (i.e., 27 A) and a constant temperature of 313 K assured by cooling water.

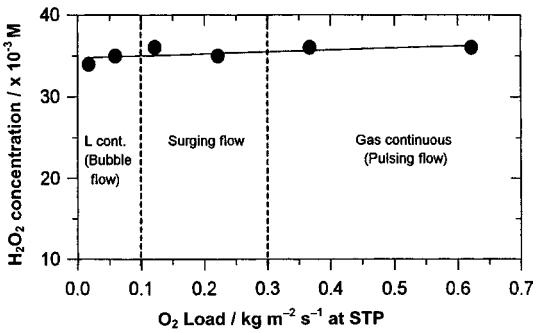

Fig. 5. The influence of flow regimes on the mediated H_2O_2 electrosynthesis at 3000 A m^{-2}. Cathode: graphite felt, liquid load 7.57 kg m^{-2} s^{-1}, O_2 pressure 0.1 MPa.

The H_2O_2 concentration, current efficiency, cell voltage and outlet pH were followed over time (Figures 6 and 7).

During the first hour of recycling (approximately 2.5 complete passes of the catholyte through the reactor), the average current efficiency was above 90% corresponding to a H_2O_2 concentration in emulsion of 0.13 M. As the recycling of the emulsion progressed without peroxide separation, the current efficiency dropped to 55% after 3 h, while the H_2O_2 concentration reached 0.24 M (Figure 6). During the first two hours the cell voltage was constant, 5.6 V and the outlet pH of the aqueous phase was between 4.5 and 5.5 (Figure 7). However, continuing the experiment, after 3 h the figures of merit deteriorated as shown by the further decline of the current efficiency (Figure 6) associated with an increase of cell voltage to 6.5 V after 5 h and outlet pH of 10. Also, a slight deterioration of the graphite felt cathode was visually observed.

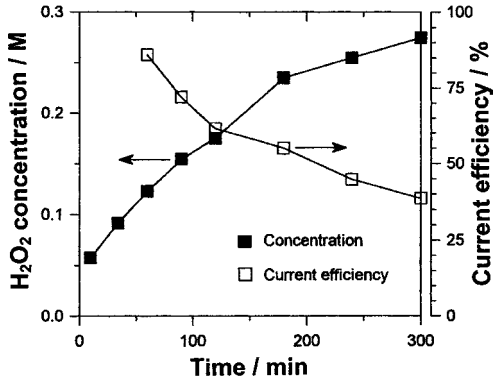

Fig. 6. Mediated electrosynthesis of H_2O_2 in a flow-by cell with complete catholyte recycle: H_2O_2 concentration and current efficiency. Cathode: graphite felt, 1000 A m^{-2}. Aqueous phase: 1 M Na_2SO_4, pH 3. Organic phase: TBP–0.2 M EtAQ–0.1 M TBAP, 10^{-3} M A336 per emulsion. Phase volume ratio: $3/1_{aq/org}$. Emulsion load 10 kg m^{-2} s^{-1}, O_2 load 0.088 kg m^{-2} s^{-1} (at STP), pressure 0.1 MPa. 313 K. Legend: (■) H_2O_2 concentration, (□) current efficiency.

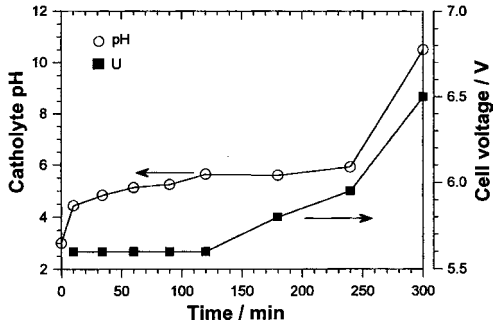

Fig. 7. Mediated electrosynthesis of H_2O_2 in a flow-by cell with complete catholyte recycle: Outlet catholyte pH and cell voltage. Cathode: graphite felt, 1000 A m^{-2}. Aqueous phase: 1 M Na_2SO_4, pH 3. Organic phase: TBP–0.2 M EtAQ–0.1 M TBAP, 10^{-3} M A336 per emulsion. Phase volume ratio: $3/1_{aq/org}$. Emulsion load: 10 kg m^{-2} s^{-1}, O_2 load 0.088 kg m^{-2} s^{-1} (at STP), pressure 0.1 MPa. 313 K. Legend: (■) cell voltage, (○) pH.

As the peroxide concentration in the emulsion exceeded the EtAQ mediator concentration from the organic phase (i.e., 0.2 M) the side reaction of H_2O_2 electroreduction gained significance, lowering the apparent current efficiency. The same effect, however, was not observed in the batch cell, where H_2O_2 concentrations up to 0.61 M were obtained with good efficiency [1]. It is likely, that the nonuniform potential and current distribution in the 0.51 m long flow cell in conjunction with the complex mass transfer effects including, the mass transport of H_2O_2 away from the electrode surface, are mainly responsible for the deterioration of the figures of merit. Furthermore, the possibility of membrane fouling due to the organic phase must be considered a factor in the increase of cell voltage. Generally, the separator performance is a challenging and crucial issue in the context of electroorganic processes [9].

4. Conclusions

The mediated electrosynthesis of H_2O_2 was investigated employing two different flow-by cells, 0.15 and 0.51 m effective length, respectively, both equipped with three-dimensional electrodes. The catholyte and anolyte solutions were 1 M and 0.5 M Na_2SO_4, respectively, acidified with glacial acetic acid to a pH of 3. The organic phase was tributylphosphate with 0.2 M 2-ethylanthraquinone (redox mediator) and 0.1 M tetrabutylammonium perchlorate (supporting electrolyte). A cationic surfactant (Aliquat® 336) was also added in concentrations up to 1 mM per emulsion. O_2 gas at 0.1 MPa was delivered with the emulsion catholyte at various loads, creating a three-phase flow.

Two types of reticulated vitreous carbon (i.e., 12 and 39 pores per cm, ppc) and graphite felt were evaluated as cathodes at superficial current densities up to 3000 A m^{-2}. The H_2O_2 concentration per pass and peroxide current efficiency generally correlated with the respective mass transfer capacities of the three-dimensional electrodes. Under the employed conditions graphite felt yielded the highest current efficiencies due to a mass transfer capacity almost an order of magnitude higher than that of RVC 12 ppc (i.e., 0.13 s^{-1} vs 0.015 s^{-1}, respectively).

Factorial experiments indicated a strong positive interaction effect between superficial current density and L/L emulsion load with respect to both current efficiency and H_2O_2 concentration. Thus, at the highest superficial current density of 3000 A m^{-2} for the lowest emulsion load (2.8 kg m^{-2} s^{-1}) the current efficiency was 18%; however, when the emulsion load was at its highest employed level (11.7 kg m^{-2} s^{-1}) the peroxide current efficiency was 84%.

Furthermore, the cationic surfactant A336 had a significant main effect and interacted also with the emulsion load. It is proposed that A336 lowers the organic phase/electrode interfacial tension thereby, en-

hancing the surface coverage by the organic phase and it also has an influence on O_2 and H_2O_2 electroreduction kinetics.

Experiments using the 0.51 m effective length cell aimed at producing high concentrations of H_2O_2 by recycling the emulsion catholyte without liquid phase and product separation, revealed a drop in peroxide current efficiency from over 90% to about 55% after 3 h when the H_2O_2 concentration reached 0.24 M. It is proposed that the competing side reaction of H_2O_2 electroreduction gained significance when the H_2O_2 concentration in emulsion exceeded the 2-ethyl-9,10-anthraquinone mediator concentration (i.e., 0.2 M). The cell voltage, between 5.6 and 6.5 V at 1000 A m^{-2}, yields a specific energy consumption of about 16 to 18 kWh $kg^{-1}_{H_2O_2}$, that is too high for industrial scale economic feasibility. Therefore, one potential area for future work should focus on lowering the energy consumption possibly by eliminating the need for a cation exchange membrane by exploring novel, undivided, cell design concepts.

Acknowledgement

The authors gratefully acknowledge the Network of Centers of Excellence (Mechanical Wood Pulps) of Canada for financial support and the University of British Columbia for awarding the University Graduate Fellowship to one of the authors (E.G.).

References

1. E.L. Gyenge and C.W. Oloman, *J. Appl. Electrochem.*, Part I, this issue (2003).
2. A. Paren and T. Tsujino, *Japan Tappi J.* **52** (1998) 630.
3. C. Oloman, M. Matte and C. Lum, *J. Electrochem. Soc.* **138** (1991) 2330.
4. 'Reticulated Vitreous Carbon', Technical Literature, ERG Materials and Aerospace Co., Oakland (1996).
5. E.L. Gyenge, 'Phase-transfer mediated electroreduction of oxygen to hydrogen peroxide in acid and alkaline electrolytes', PhD dissertation, The University of British Columbia, Vancouver, Canada (2001).
6. F. Kraft, *in* R.G. McDonald and J.N. Frankin (Eds), 'Pulp and paper manufacture', Vol. 1 (McGraw-Hill, New York, 2nd edn, 1969), pp. 723–724.
7. A. Storck, M.A. Lafiti, G. Barthole, A. Laurent and J.C. Charpentier, *J. Appl. Electrochem.* **16** (1986) 947.
8. I. Hodgson and C. Oloman, *Chem. Eng. Sci.* **54** (1999) 5777.
9. D. Danly and C.R. Campbell, *in* N.L. Weinberg and B.V. Tilak (Eds), 'Technique of Electroorganic Synthesis. Part III: Scale-up and Engineering Aspects', (J. Wiley & Sons, New York, 1982), pp. 283–340.
10. R.C. Reid, J.M. Prausnitz and T.K. Sherwood, 'The Properties of Gases and Liquids', (McGraw-Hill, New York, 3rd edn, 1977).
11. J.M. Fenton and R.C. Alkire, *J. Electrochem. Soc.* **135** (1988) 2200.
12. D. Schmal, J. van Erkel and P.J. van Duin, *J. Appl. Electrochem.* **16** (1986) 422.
13. K.M. Takahashi and R.C. Alkire, *Chem. Eng. Commun.* **38** (1985) 209.
14. A.I. Masliy and N.P. Podubbny, *J. Appl. Electrochem.* **27** (1997) 1036.
15. C. Oloman, *J. Electrochem. Soc.* **126** (1979) 1885.

Appendix 1: Estimation of the organic liquid to solid mass transfer coefficient, mass transfer capacity, maximum electroactive bed thickness and limiting current density for co-current upward three-phase (L/L/G) flow in graphite felt and reticulated vitreous carbon electrodes

There are no mass transfer correlations in the literature for three-phase flow through three-dimensional fibre bed electrodes. Extrapolation of existing mass transfer correlations determined for *cm* and *mm* packing sizes, to fibre beds with characteristic diameters the order of *μm*, is unwarranted.

An estimation of the organic liquid to solid mass transfer capacity was attempted for the present conditions by applying certain approximations to available single and two-phase flow data for graphite felt and reticulated vitreous carbon electrodes. In this respect, the acidic emulsion was treated as one entity characterized by an overall conductivity of 2.3 S m^{-1} [1], and average viscosity of 2.23×10^{-3} Pa s (calculated as a function of the pure component viscosities and volume fractions [10]).

The one-phase liquid to solid mass transfer coefficient for RVC (established for an 18 pores per cm electrode) is given by [11]:

$$Sh = 11 \times Re^{0.3} \tag{A1}$$

where

$$Sh = \frac{K_{0,\mathrm{RVC}} \times \varepsilon}{a_{\mathrm{org}} \times D_{\mathrm{EtAQ}}} \tag{A2}$$

and

$$Re = \frac{u_0}{a_{\mathrm{org}} \nu_{\mathrm{k}} \varepsilon} \tag{A3}$$

where a_{org} is the specific surface area available for the organic phase ($m^2\ m^{-3}$), D_{EtAQ} the diffusion coefficient of EtAQ in TBP (1.5×10^{-10} $m^2\ s^{-1}$ [5]), $K_{0,\mathrm{RVC}}$ the organic liquid to solid (RVC) mass transfer coefficient ($m\ s^{-1}$), ν_{k} the kinematic viscosity of the emulsion (2.23×10^{-6} $m^2\ s^{-1}$), u_0 the linear velocity of the emulsion (4×10^{-3} m s^{-1} for the case presented in Figure 4), and ε the effective bed porosity for the liquid phase. The latter is expressed as

$$\varepsilon = \varepsilon_{\mathrm{m}} \times \beta_{\mathrm{L}} \tag{A4}$$

where β_{L} is the liquid-hold up and ε_{m} the matrix porosity (Table 1).

The liquid hold-up can be expressed as [8]:

$$\beta_L = 1 - 0.907L^{-0.362}G^{0.301} \quad \text{(A5a)}$$

$$0 < G < 0.35\,\text{kg m}^{-2}\text{s}^{-1} \quad \text{(A5b)}$$

$$1.53 < L < 7.62\,\text{kg m}^{-2}\text{s}^{-1} \quad \text{(A5c)}$$

where G is the O_2 gas load at STP (kg m^{-2} s^{-1}) and L is the emulsion load (kg m^{-2} s^{-1}).

In applying Equation A2 it was assumed that a_{org} is proportional to the volume fraction of the organic phase f_{org}, according to Equation A6:

$$a_{org} = f_{org} \times a_m \quad \text{(A6)}$$

where a_m is the specific surface area of the three-dimensional matrix (m^2 m^{-3}) (Table 1).

In the case of graphite felt electrode the one-phase liquid to solid mass transfer coefficient is given by [12]:

$$Sh = 7 \times Re^{0.4} \quad \text{(A7)}$$

where

$$Sh = \frac{K_{0,GF} \times d_f}{D_{EtAQ}} \quad \text{(A8)}$$

and

$$Re = \frac{u_0 \times d_f}{\nu_k} \quad \text{(A9)}$$

where $K_{0,GF}$ organic liquid to solid (GF) mass transfer coefficient (m s^{-1}) and d_f is the graphite fibre diameter (2×10^{-5} m). The rest of the variables have the meaning as discussed before.

Substituting into Equations A1–A9 one obtains $K_{0,RVC}$ and $K_{0,GF}$. Furthermore, one has to take into account the influence of the O_2 gas flow ('reactive' flow) on the liquid to solid mass transfer. For vitreous carbon electrodes operated in bubble flow regime the presence of gas phase increased the mass transfer coefficient over the corresponding coefficient for one-phase flow by a factor of 1.7 [13]. For graphite felt electrodes, extrapolating the literature data for the liquid and gas loads employed in the case discussed by Figure 4, suggests an enhancement of the single-phase mass transfer coefficient by a factor of 1.5–1.7 [8].

Therefore, the overall liquid to solid mass transfer coefficient for EtAQ electroreduction in the presence of O_2 gas flow K, is

$$K_j = 1.7\,K_{0,j} \quad \text{(A10)}$$

where j index refers to either RVC or GF.

Finally, the mass transfer capacity K_{mc} (s^{-1}) is given by

$$K_{mc,j} = a_{org} \times K_j \quad \text{(A11)}$$

For the experimental conditions associated with Figure 4 (Section 3.1), K_{mc} is presented in Table 2.

For the present case of solid matrix electronic conductivity σ much greater than the electrolyte conductivity κ (e.g., about ten times in the case of GF and sixty times for RVC 12 ppc) the maximum electroactive bed thickness τ (m) is expressed by [14, 15]:

$$\tau = \left(\frac{2\kappa_{em,eff}\Delta\Phi_{max}}{nFK_{mc}C_{EtAQ}}\right)^{1/2} \quad \text{(A12)}$$

with

$$\kappa_{em,eff} = \frac{2\kappa_{em}\varepsilon}{3 - \varepsilon} \quad \text{(A13)}$$

where n total number of electrons involved in EtAQ electroreduction (=2), $\Delta\Phi_{max}$ maximum allowable potential drop (V) for which side reactions such as H_2O_2 electroreduction are avoided (i.e., width of the limiting current plateau), κ_{em} and $\kappa_{em,eff}$ emulsion [1] and effective emulsion conductivity (S m^{-1}). Based on EtAQ and H_2O_2 electroreduction experiments [5], $\Delta\Phi_{max}$ was assumed equal to 0.15 V.

The maximum electroactive bed thickness calculated with Equations A12–A13 is also given in Table 2.

The mass transfer limited current density for EtAQ reduction i_{ml} (A m^{-2}) is related to the mass transfer capacity, maximum electroactive bed thickness τ (m), and EtAQ concentration C_{EtAQ} (mol m^{-3}) as follows:

$$i_{ml} = 2\,FK_{mc}\tau C_{EtAQ} \quad \text{(A14)}$$